A human organoid system that self-organizes to recapitulate growth and differentiation of a benign mammary tumor

Stefan Florian[a,b,1], Yoshiko Iwamoto[c], Margaret Coughlin[a], Ralph Weissleder[a,c], and Timothy J. Mitchison[a,1]

[a]Department of Systems Biology, Harvard Medical School, Boston, MA 02115; [b]Institute of Pathology, Charité University Hospital, 10117 Berlin, Germany; and [c]Center for Systems Biology, Richard B. Simches Research Center, Massachusetts General Hospital, Boston, MA 02114

Contributed by Timothy J. Mitchison, April 12, 2019 (sent for review February 13, 2017; reviewed by Mina J. Bissell and Andrew J. Ewald)

As 3D culture has become central to investigation of tissue biology, mammary epithelial organoids have emerged as powerful tools for investigation of epithelial cell polarization and carcinogenesis. However, most current protocols start from single cells suspended in Matrigel, which can also restrict cell differentiation and behavior. Here, we show that the noncancerous mammary cell line HMT-3522 S1, when allowed to spontaneously form cell aggregates ("spheroids") in medium without Matrigel, switches to a collective growth mode that recapitulates many attributes of "usual ductal hyperplasia" (UDH), a common benign mammary lesion. Interestingly, these spheroids undergo a complex maturation process reminiscent of embryonic development: solid-cell cords form their own basement membrane, grow on the surface of initially homogeneous cell aggregates, and form asymmetric lumina lined by two distinct cell types that express basal and luminal cytokeratins. This sequence of events provides a cellular mechanism that explains how the characteristic crescent-shaped, asymmetrical lumina form in UDH. Our results suggest that HMT-3522 S1 spheroids are useful as an in vitro model system to study UDH biology, glandular lumen formation, and stem cell biology of the mammary gland.

epithelial tube | mammary gland | organoids | lumen formation | usual ductal hyperplasia

The mammary gland is a branched tubular organ. Its epithelial tubes form through central perforation of solid-cell cords and are lined by bilayered epithelium (1, 2) consisting of a basal cell layer that secretes basement membrane components and an apical cell layer lining the lumen. It is unique in that it undergoes two distinct phases of development: embryonic—when tubes are formed de novo—and postnatal during puberty and pregnancy—when the initially rudimentary tubular system grows and matures and milk-secreting acini (or alveoli) form at the duct ends.

In 3D culture systems of epithelial cells, tissues can be grown in gels that model ECM and stroma or as cell aggregates floating in medium. Normal mammary epithelial cells are usually cultured in or on gels. A frequently used protocol involves seeding of single cells in Matrigel (ECM extracted from Engelbreth–Holm–Swarm mouse sarcoma) (3). Under these conditions, individual epithelial cells distributed throughout the gel will proliferate and form a rudimentary spherical glandular structure called an "acinus" that consists of a monolayer of polarized epithelial cells that are separated from the surrounding Matrigel by a basement membrane. The apical side of the cells is oriented toward the center of the acinus that can contain a hollow lumen. This model has been used extensively to study the role of ECM in cell polarization and cancer development as well as the role of oncogenes in cancer initiation (4, 5). However, this artificial monolayered epithelium fails to recapitulate the collective processes that occur during mammary gland development or regeneration and does not form bilayered epithelium. Therefore, models that emulate formation of multilayered breast epithelium use preformed pieces of bilayered epithelium isolated from mouse mammary glands (6–8) or whole-gland explants as starting material. These fragments, when seeded into gel substrates, will form epithelial tubes through branching morphogenesis, a process that involves collective outgrowth and branching of epithelial cell cords, followed by spontaneous lumen formation in the cord center.

Here, we introduce a Matrigel-free culture approach for the HMT-3522 S1 mammary cell line isolated from a patient with a benign breast lesion. It results in the differentiation and spatial organization of an initially homogeneous mix of cells into multilayered epithelium with a spontaneously forming basement membrane and a lumen. This process requires collective coordination of cellular behavior and involves a complex, multistage process that involves several steps reminiscent of embryonic mammary development. At each stage of this process, this cell line reproduces morphological hallmarks of usual ductal hyperplasia (UDH), including formation of lumina lined by nonpolarized epithelial cells, a basement membrane, and multilayered epithelium reminiscent of normal mammary epithelium.

UDH (also known as conventional ductal hyperplasia or epitheliosis) (9–12) is a benign proliferation of mammary epithelium that emerges mostly in peripheral ducts of the adult mammary gland, filling up the luminal space. It is associated with an 1.5–2 times increased risk of breast cancer (13), but as opposed to other benign lesions, it is not considered a direct precursor lesion of breast cancer. It does not require any therapy, is

Significance

Organoid culture allows the study of tissue function and development in vitro. Here, we show that mammary cells can autonomously reassemble in vitro to form a common benign mammary lesion [usual ductal hyperplasia (UDH)]. Currently, very little is known about how UDH develops. In vitro, we observe a coordinated process reminiscent of embryonic development of the mammary gland that recapitulates typical morphological hallmarks of UDH at all stages, suggesting that, in vivo, such lesions also form through the same sequence of events. Thus, we speculate that UDH lesions form through activation of embryonic-like developmental programs in adult mammary cells. The culture protocols introduced here will be useful to study supracellular coordination of mammary cell behavior.

Author contributions: S.F. designed research; S.F., Y.I., and M.C. performed research; S.F. analyzed data; and S.F., R.W., and T.J.M. wrote the paper.

Reviewers: M.J.B., E. O. Lawrence Berkeley National Laboratory; and A.J.E., Johns Hopkins University.

The authors declare no conflict of interest.

[1]To whom correspondence may be addressed. Email: stefan.florian@charite.de or timothy_mitchison@hms.harvard.edu.

This article contains supporting information online at www.pnas.org/lookup/suppl/doi:10.1073/pnas.1702372116/-/DCSupplemental.

Published online May 17, 2019.

not palpable, and is a random finding in ~25% of breast biopsies. At the cellular level, it is a proliferation of both basal and apical cell precursors arranged in a typical "mosaic"-like pattern. No consistently occurring driver mutations are known for this lesion, which is diagnosed by its characteristic histological appearance.

Based on our results, we hypothesize that UDH and mammary embryonic development might be caused by (re-)activation of similar developmental programs and postulate that HMT-3521 S1 spheroids are closely emulating this program in vitro.

Results

Differentiation of a Breast Epithelial Cell Line in Spheroid Culture. This project was triggered by our interest in generating normal and malignant mammary spheroids for comparative testing of cancer drugs. Spheroid culture (14) is frequently used in developmental biology (embryoid bodies, gastruloids), cancer drug testing, and toxicology but had not, to our knowledge, been tested as a culture approach for normal mammary cells. Therefore, we asked whether mammary epithelium can form in vitro without the cues provided by the ECM components found in Matrigel. We used the well-characterized "normal" mammary epithelial cell line HMT-3522 S1 (15). This line was isolated from a benign breast lesion from a healthy donor and maintains several properties of normal cells, like contact inhibition and the abilities to polarize, differentiate, and secrete milk proteins. It has been widely used to study mammary gland biology in Matrigel-based 3D culture (5). We used the same serum-free culture medium of defined composition (3), but instead of dispersing single cells in Matrigel, we plated ~10^4 cells into commercially available round-bottom, nonadherent plastic plates.

Under spheroid culture conditions, HMT-3522 S1 cells formed tight, spherical aggregates within 2–3 d (Fig. 1*A*). All cells showed positive staining with a pancytokeratin antibody (Fig. 1*A*), confirming the epithelial origin of this cell line. At this early stage, HMT-3522 S1 cells expressed cytokeratin 14 (CK14), a high-molecular weight keratin expressed in basal and precursor cells of normal mammary epithelium, in a mosaic-like expression pattern that is typical for UDH (16). The luminal marker CK8 was also expressed in some randomly distributed cells in line with the characteristic mixed basal/luminal cell composition of UDH.

During the next 2–3 wk, the initially homogeneously mixed cell population developed into structures with two clearly distinguishable zones (Fig. 1*B*): a densely packed central core that maintains the morphology of the initial culture days and a peripheral zone with more sparsely distributed nuclei and larger, often elongated cells connected to each other through densely distributed desmosomes (*SI Appendix*, Fig. S1).

Self-Organized Outgrowth of Solid Cords. Also within the first 2 wk, a front of cells consisting of the same two cell types "breaks out" from the spheroid and grows on its surface, resulting in formation of a cell layer that is concentric with the spheroid (Figs. 1*B* and 2 and Movie S1). The layers are separated by laminin, a basement membrane component that is autonomously deposited by the cells (Fig. 1*B*). In stark contrast to the cells in the original

MEDICAL SCIENCES

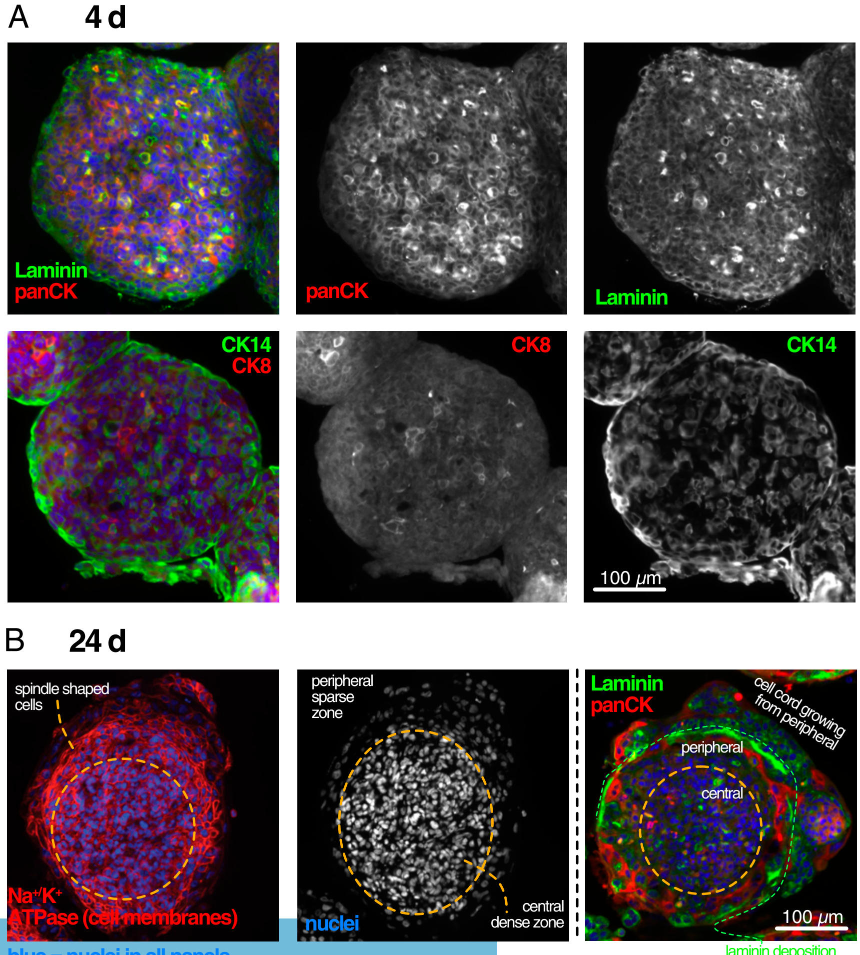

Fig. 1. Young spheroids consist of two cell types and form two distinct zones. (*A*) A 4-d-old spheroid stained for laminin, pancytokeratin (panCK), the basal cell marker CK14, and the luminal cell marker CK8. (*B*) A 24-d-old spheroid stained for the cell membrane marker Na^+/K^+ ATPase, laminin, and panCK. Nuclei are counterstained with DAPI.

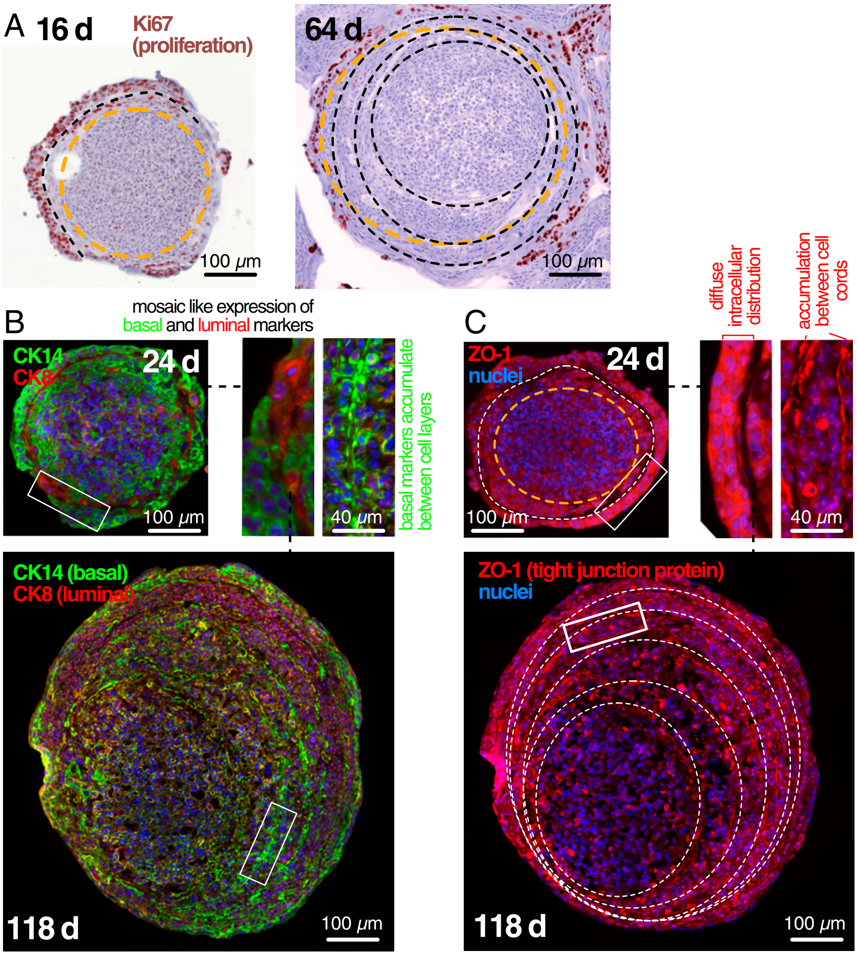

Fig. 2. Cell cords grow on the spheroid surface and form concentric circles with basal expression of CK14. (*A*) Comparison of 16- and 64-d-old spheroids shows growth through progressive accumulation of concentric cell cords. Note that proliferation occurs only in the most peripheral layer outside of the orange circle. Black dashed lines show boundaries between layers. (*B* and *C*) Comparison of 24- and 118-d-old spheroids shows that initially diffusely distributed CK14 (basal epithelial marker)-expressing cells accumulate at the periphery of cell cords along with the tight junction protein ZO-1. Dashed white lines indicate boundaries between layers.

spheroid center, most of these protruding cells proliferate as evidenced by a positive Ki67 staining (Fig. 2*A*). After a layer is completed, the growing cords move outward to the next level and generate the next concentric layer of similar thickness. Viewed in cross-section, the resulting picture is reminiscent of the layers of an onion. Within these concentric layers, the initially uniform mix of heterogeneous cells eventually polarizes and forms two zones (Fig. 2*B*): a zone of $CK14^+/CK8^+$ (luminal markers) cells within the circles and a zone of $CK14^{++}/laminin^+$ cells (basal and basement membrane markers) at the medium-facing periphery of each circle, which separates each concentric circle from its outer neighbor. The initially uniformly distributed tight junction protein ZO-1, found on the apical cell membranes at the sites of lumen formation during normal mammary embryonic development (7), also accumulates between layers (Fig. 2*C*).

Matrigel Interferes with Initial Solid-Cord Formation. When we transferred preformed unattached spheroids from medium into Matrigel, we found that cell cords start to grow perpendicularly into the surrounding ECM from the smooth spheroid surface instead of forming concentric layers, similar to the glandular tree forming cell cords growing from the primary bud during embryonic development of the mammary gland (Fig. 3 *A*–*C*). Interestingly, however, this only occurs if spheroids are transferred to Matrigel at least 6 d after plating. If transfer is performed earlier, no cell cords are visible, and spheroids grow through division of homogeneously distributed cells around their whole surface through formation of small cell clusters the size of classic HMT-3522 S1 acini (5) (Fig. 3*D*). In line with this observation, in 4-d-old spheroids kept in medium (Fig. 3*E*), proliferation is higher and occurs diffusely throughout the spheroid compared with 24-d-old spheroids, where growth is relatively low and limited to the cell cords protruding from the surface at the spheroid periphery (Fig. 3*F*). These observations suggest that, at day 5/6 after plating, a switch to collectively coordinated growth occurs in the spheroids that enables cell cord formation. This switch is inhibited but cannot be reversed by contact to Matrigel.

Bilayered Epithelium Lining an Open Surface Forms Through Apical Detachment. At ∼3.5 mo after plating, most spheroids have accumulated several layers of cell cords separated by focused layers of laminin, a component of basement membranes (Fig. 4*A*). Next, cell cords detach spontaneously from each other, resulting initially in the formation of small cavities (Fig. 4 *B* and *C*) that later grow and converge into larger communicating spaces lined on one side by a basal layer of cells on a layer of laminin and on the other side by "apical cells" facing the lumen (Fig. 4 *C*–*E*). The laminin bridges sometimes spanning the lumen between separated cell layers (Fig. 4*D*) suggest that, similar to lumen formation during the formation of tubes in embryonic development, these spaces form through a process that pushes or pulls the cells apart. In contrast to embryonic glandular tube formation, however, where the lumen forms between two apical surfaces at the center of a cord, these lumina form between cell cords and are asymmetrically lined by apical cells on one side and basal cells on the other side instead of two facing layers of apical cells (Fig. 4 *D* and *E*). Probably as a result of this nonphysiological lumen formation process, the tight junction marker ZO-1 is mislocalized and remains associated with the laminin

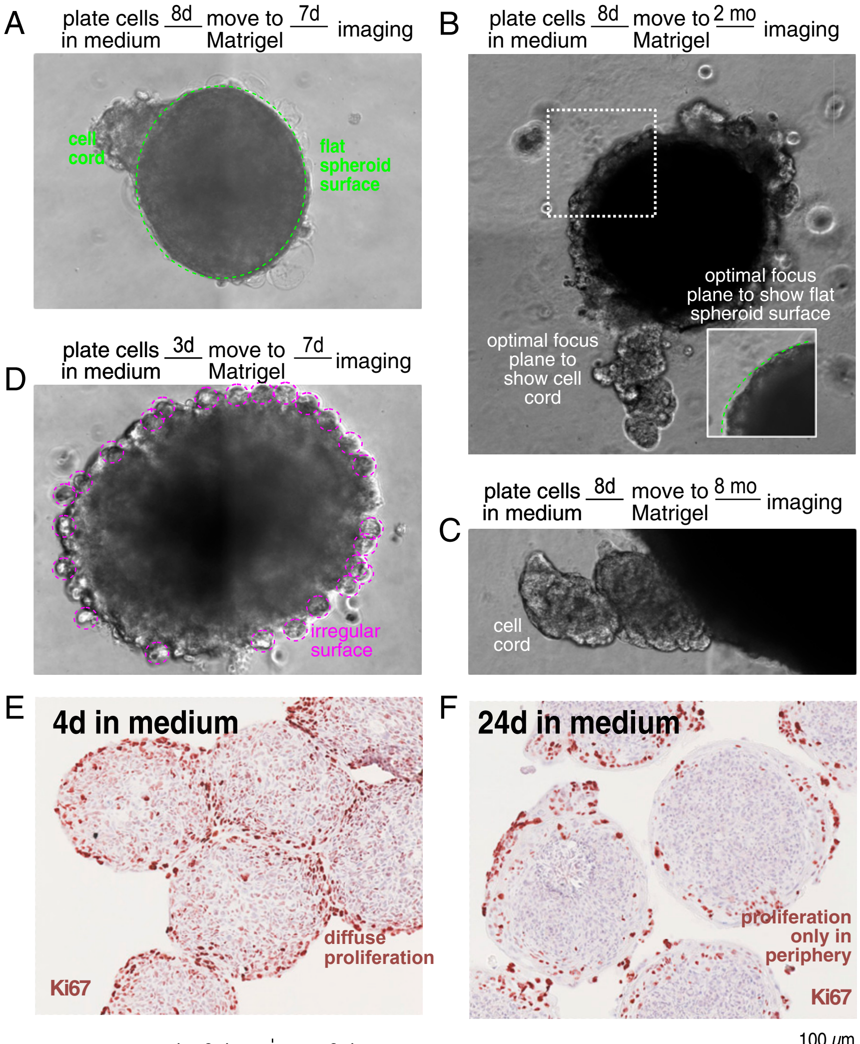

G

	under 6 days irregular surface		over 6 days flat surface				
Time in medium (days)	3	**5**	**6**	7	8	215	394
no. of spheroids analyzed	2	3	1	3	4	1	1

Fig. 3. A switch to collective cell behavior on day 5/6 after spheroid formation. (*A–D*) Phase contrast images of spheroids taken after 8 or 3 d in medium (as indicated) followed by 7 d, 2 mo, or 8 mo in Matrigel (as indicated). (*E* and *F*) Ki67 staining of spheroids grown in medium for 4 and 24 d, respectively. Note the switch from a homogeneous, diffuse localization of proliferating cells to a peripheral zone. (*G*) Overview of phenotype of all spheroids that were transferred from medium to Matrigel.

layer rather than the apical side of the cells lining the lumen (Fig. 4*F*).

From 5.5 to 8 mo after plating, after lumen formation is completed, the cell cords form a progressively thinner epithelium (eventually reaching a thickness of two to four cell layers), delimited on the apical (central) side by the lumen and on the basal (peripheral) side by a basement membrane (BM) (Fig. 4*D*).

In summary, spheroids formed from the HMT-3522 S1 normal mammary cell line form solid-cell cords that protrude from an initial cell aggregate, and these cords give rise to multilayered, sometimes bilayered, epithelium with a basement membrane and a lumen, with basal cells correctly expressing higher levels of CK14. The crescent-shaped lumen is asymmetric, lined by a layer of basal cells on one side and unpolarized apical cells on the other that fail to form proper tight junctions.

Epithelial Morphogenesis in Spheroids Is a Highly Reproducible, Collective Process. Morphogenesis of HMT-3522 S1 aggregates was reproducible and robust (Fig. 5). Of 58 spheroids that were grown in individual wells for this study, only 3 (5%) showed major deviations from the morphology, timing, and sequence of events described above. Fig. 5*A* shows that spheroids of the same age almost invariably had the same number of layers. The switch from degenerating basal syncytia (Fig. 5*A*, orange lines) to apical detachment and formation of microlumina after the BM had matured occurred at ~100-d spheroid age, and first regions of bilayered epithelium were observed at ~150 d. Inconsistent feeding delayed formation of BM and led to formation of spheroids that show both zones that have reached the luminal detachment stage and others where the BM is still forming but the differentiation process per se still took place (Fig. 5, three data points at 118 d). While the number of very old spheroids analyzed here is relatively low, it is still interesting that, while old spheroids added new layers more and more slowly, seemingly reaching a plateau (Fig. 5*A*), spheroid volume grew linearly over time. This is in line with the hypothesis that these spheroids grow through elongation of "crawling" cell cords at a constant speed independent of the surface area or the volume of the spheroid. This growth pattern is fundamentally different from growth of tumor spheroids, which grow through constant apposition of new

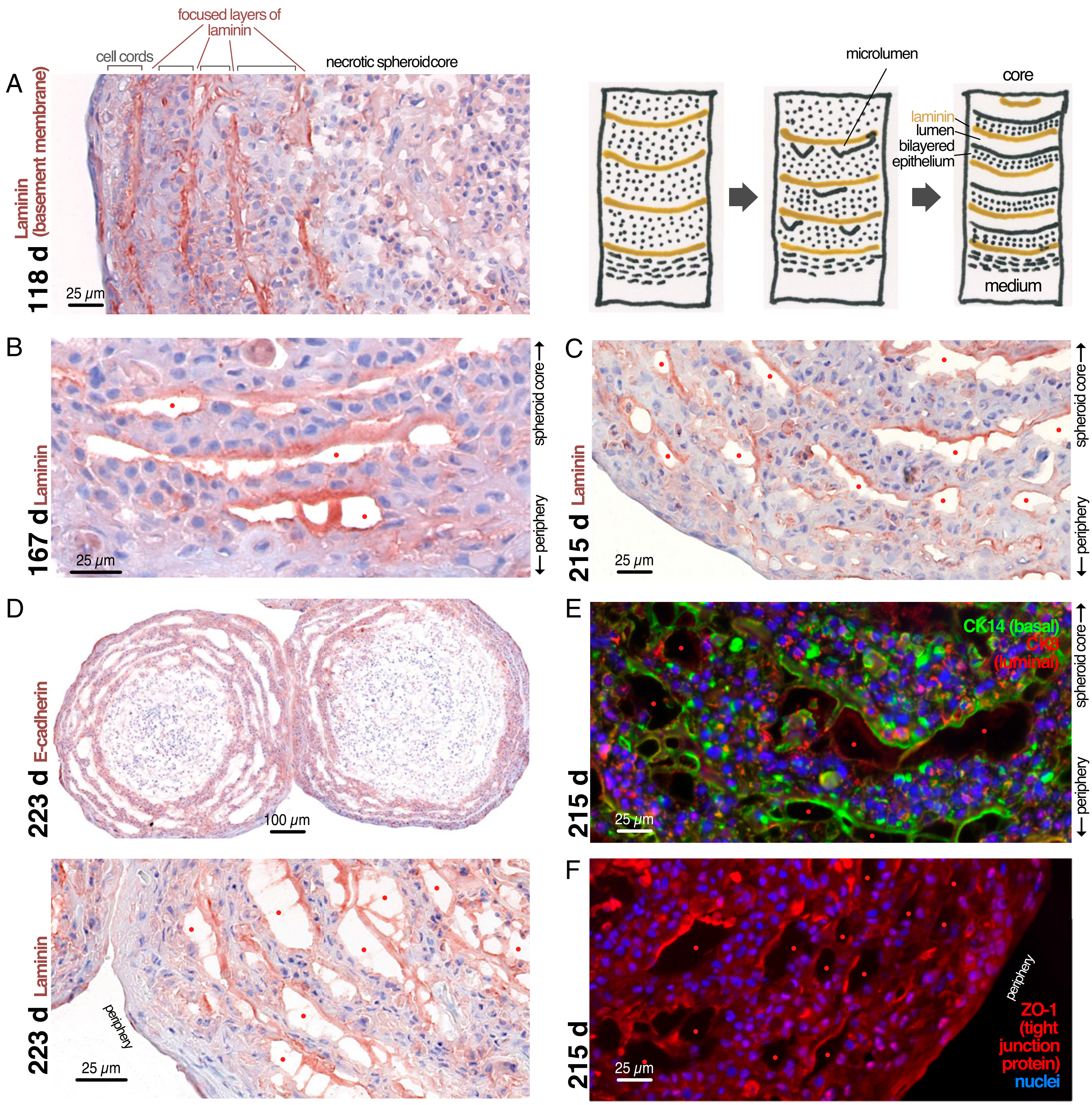

Fig. 4. Concentric cell cords detach from each other to form asymmetric, slit-like lumina and rudimentary breast epithelium. (*A–F*) Spheroids were grown in medium for the indicated number of days and stained by immunohistochemistry or immunofluorescence for laminin, E-Cadherin, CK14, or ZO-1 as indicated. Red dots: slit-like lumina.

cells all over the spheroid surface and characteristically have a growth curve that follows a sigmoid Gompertz function (17).

UDH as the Result of a Four-Stage Developmental Process. Interestingly, the morphology of these spheroids at all developmental steps is very similar to a frequent benign breast lesion known as UDH. UDH [or conventional ductal hyperplasia, also known as epitheliosis (9–11)] is a benign proliferation of mammary epithelium that emerges in peripheral ducts of the adult mammary gland, filling up the luminal space. It is characterized by four architectural principles (12): central cell masses with peripheral, crescent-shaped spaces ("fenestrations"); a parallel arrangement of cell nuclei that results in a "streaming" picture; a central, denser core with overlapping nuclei and looser arrangement of cells in the periphery ("maturation phenotype"); and finally, nuclear shapes that vary "from elongated through oval to reniform, folded, or convoluted and usually do not appear round and never look uniform."

Cells often have indistinguishable cell borders, giving the impression of a syncytium. In complex lesions, they can "grow as mounds and stream in a circular direction, producing concentric layers, which suggest the appearance of the cut surface of an onion"

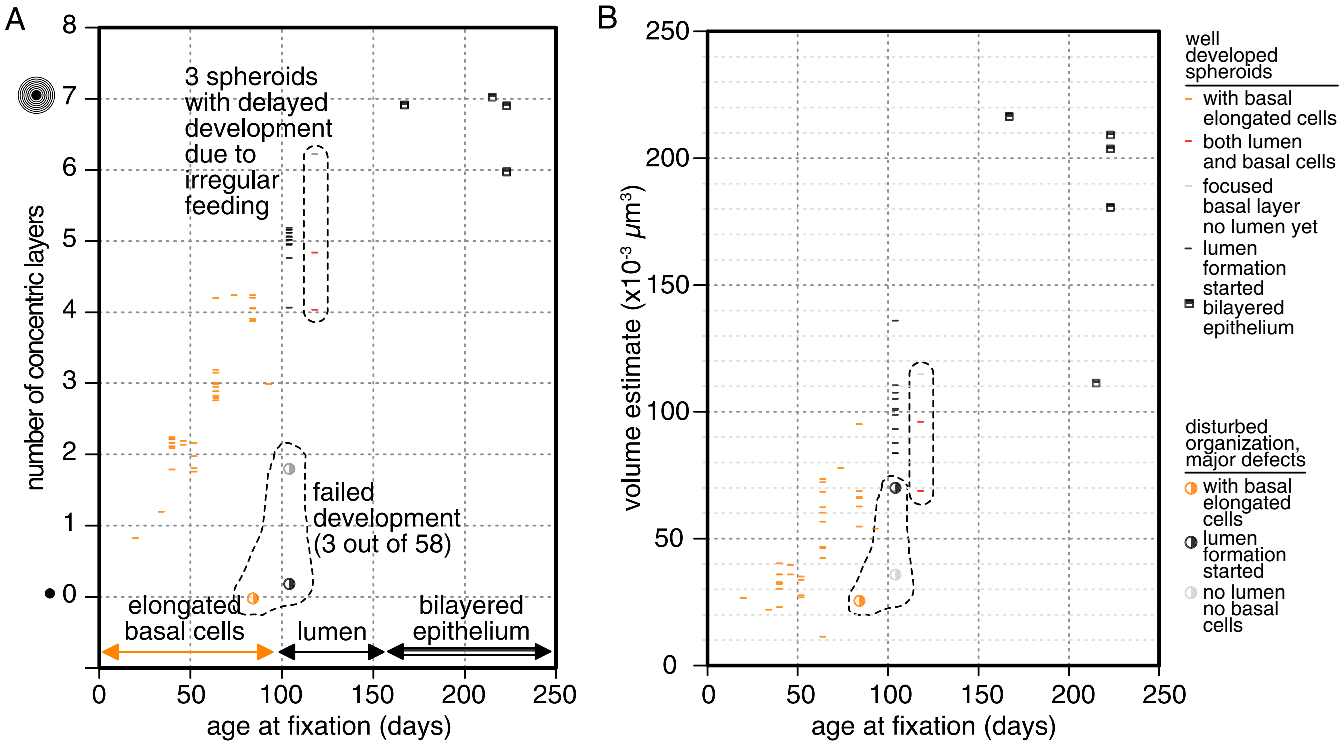

Fig. 5. Spheroids maturation is highly reproducible. Quantitative analysis of all HMT-3522 S1 spheroids analyzed in this study. In *A*, spheroid age is plotted against the number of concentric cell layers surrounding the original core spheroid. Because the number of layers is a discrete variable, a low amount of random jitter was introduced in this dimension to make each data point visible. In *B*, spheroid age is plotted against spheroid volume as estimated by calculating the spheroid radius from the area of the histology section. The whole dataset contains 58 spheroids, with each symbol corresponding to 1 spheroid.

(12). Importantly, not all architectural features that are characteristic for UDH need to occur simultaneously in a single lesion. UDH is a mix of basal precursor cells positive for CK5/CK6 (and their partner CK14) and luminal cells positive for CK18, resulting in a typical "mosaic-like" staining pattern for these proteins (16).

Our spheroids go through four different developmental stages that, taken together, show all of the features mentioned above. The typical morphological features of UDH and corresponding developmental stages of HMT-3522 S1 spheroids are listed in Table 1. Figs. 6 and 7 show examples of UDH and their similarities with spheroids.

Taking into account that the HMT-3522 cell line was generated from a benign fibrocystic breast lesion containing papillomas (15) (which often occur in connection with UDH), we believe that our in vitro culture system represents a UDH lesion growing in absence of surrounding stroma or ducts. Since stroma plays an essential role both for embryonic development and for tumor development in glandular organs (20, 21), it is astonishing that this highly coordinated process can take place without any supporting stroma or exogenous ECM. Presumably, this is possible with UDH cells, because also in vivo, they grow inside a hollow lumen without direct contact to the original basement membrane or stroma, which is not the case for malignant tumors.

Discussion

The causes and biological mechanisms behind UDH development have so far remained elusive, and no characteristic mutations for this lesion have been found. The characteristic mix of two cell lineages (basal and luminal) observed in UDH distinguishes it from precancerous lesions and invasive breast cancers, which are characterized by expansion of just one cell type. The landmark morphological and differentiation features of UDH have been traditionally described without an understanding of their biological relationship to each other, and it is not clear if, for example, the maturation phenotype represents an early stage of UDH or an alternative manifestation to the fenestration phenotype with slit-like lumina. Assuming that spheroids indeed

Table 1. Developmental stage of spheroids and the corresponding morphological hallmarks of UDH

Stage of development of spheroid	Morphological hallmark of UDH
Freshly formed spheroid (Fig. 1*A*)	Mosaic-like staining pattern CK14/CK8 (16)
Two-zone spheroid (Fig. 1*B*)	Maturation phenotype, irregular nuclear spacing, syncytia, streaming, nuclear shape (12), mosaic-like pattern CK14/CK8
Concentric layers formed by cell cords without lumen (Figs. 2 and 3)	Concentric growth of solid-cell cords (12), mosaic-like pattern of CK14/CK8 (16)
Multilayered epithelium with lumen (Fig. 4)	Fenestrations (slit-like lumina) with peripheral epithelium and convex border with myoepithelial layer (18), apocrine tufts or snouts (9), basal myoepithelial layer, continuous lumina (19)

All: nuclear indentation (12).

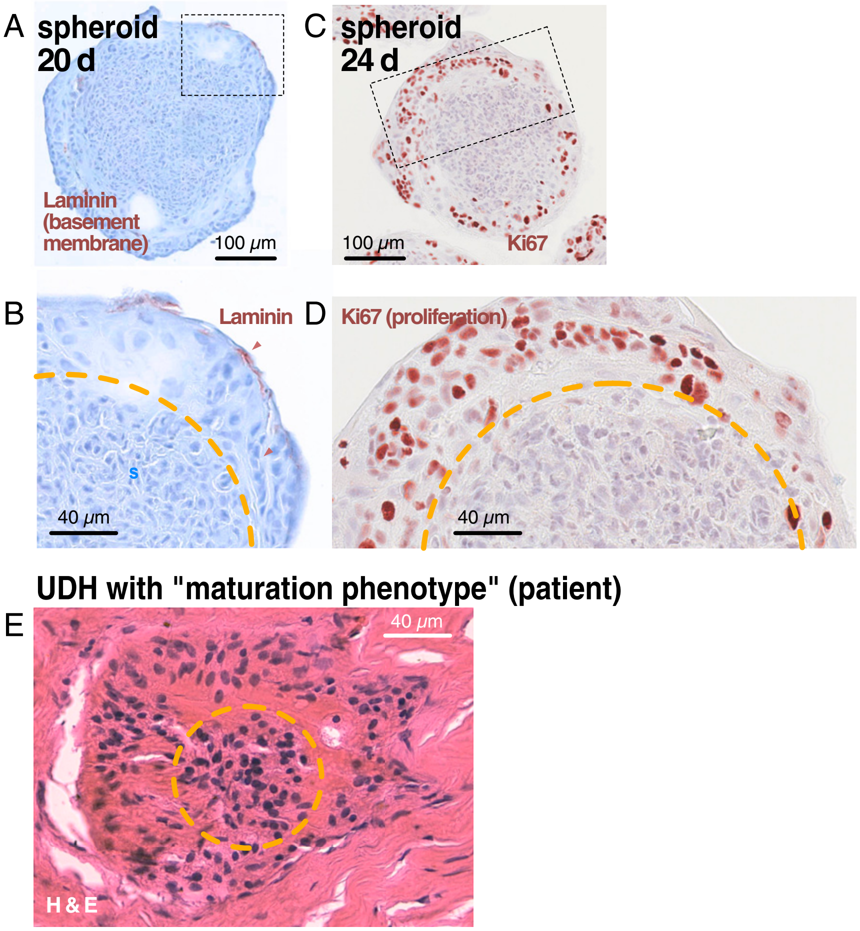

Fig. 6. Similarities in morphology of young spheroids and UDH with "maturation" phenotype. (*A–D*) A 20-d-old spheroid and a 24-d-old spheroid stained for laminin and Ki67, respectively. Note the clear separation between central and peripheral zones. In the peripheral zone, cells deposit laminin at the periphery and proliferate, being surrounded by a pale, hyaline substance with indistinguishable cell borders (compare with Fig. 1*B*). (*E*) Small focus of UDH from a patient featuring a maturation phenotype. This name is based on the assumption in the literature that the peripheral, more pale nuclei surrounded by hyaline substance represent cells that undergo a maturation process and become more differentiated toward the lesion center. Our spheroid results suggest that, instead, the peripheral cells are derived from and grow out from the core. The orange line marks the border between dense central and loose peripheral zones.

recapitulate the development of UDH in vitro, their highly reproducible, synchronous development provides an unique opportunity to observe the formation of these benign lesions longitudinally over time, which would be very hard to do in patients. Our observations in spheroids surprisingly suggest that UDH lesions emerge through a highly coordinated differentiation process that culminates in formation of rudimentary mammary epithelium, and the different known manifestations constitute different stages along this process.

Relationship of UDH to Embryonic Mammary Development. Moreover, our spheroid model suggests that formation of UDH lesions has several similarities to embryonic development of the mammary gland. Starting from a central bud, embryonic gland ducts form a tree through branching of cell cords that eventually gain a lumen (22). This primary bud consists of a mix of mainly CK14-positive and at least in the mouse, some CK8-positive cells that eventually differentiate into two cell types expressing basal and apical cell markers (23–26). Furthermore, according to the limited literature on embryonic development of the human mammary gland (27–29), the timing of the different stages that we observe in spheroid development is very similar to the development timeline in vivo (*SI Appendix*, Fig. S2). Considering that UDH lesions can form new (rudimentary) mammary epithelium that lies within the lesion and is distinct from original epithelium lining the duct from which the lesion has emerged (Fig. 7) (9), it seems likely that the epithelium lining the typical asymmetrical lumina is the result of a differentiation process reminiscent of embryonic mammary development.

Lumen Formation as an Active Process in UDH. However, embryonic development is in two ways fundamentally different from spheroids (and UDH): during embryonic development, cell cords grow perpendicularly to the central bud surface (not concentrically), and the lumen forms in the cord center rather than on its side. In Fig. 3, we have shown that, given a semisolid, ECM-rich Matrigel environment, cell cords growing from spheroids also have the ability to grow perpendicularly and invade the surrounding ECM, suggesting that the concentric growth pattern is due to the lack of physical support through surrounding stroma. The differences in lumen formation, however, are more complex and raise a number of interesting questions, which might be addressed using spheroids:

One question is how the slit-like lumina observed in UDH form. They are a hallmark of this lesion, often lined by a smooth convex side with flattened cells and nuclei aligned along the luminal border facing a concave side with "nonpolarized glandular cells" (Fig. 7). Different explanations for this characteristic shape and how these lumina are formed have been suggested, but it has so far remained unclear if they result from an active lumen formation process or simply constitute empty space that has not yet been filled up by epithelial masses that grow into the duct lumen (12). It has also been suggested that UDH might contain two types of lumina that are not connected to each other. Under this model, peripheral lumina would constitute void ductal space, and the more central ones called "secondary fenestrations" would result from an active process of lumen formation. However, 3D reconstruction studies of patient lesions have shown that, in UDH, as opposed to malignant tumors, lumina invariably form an interconnected network of hollow spaces (19). Assuming

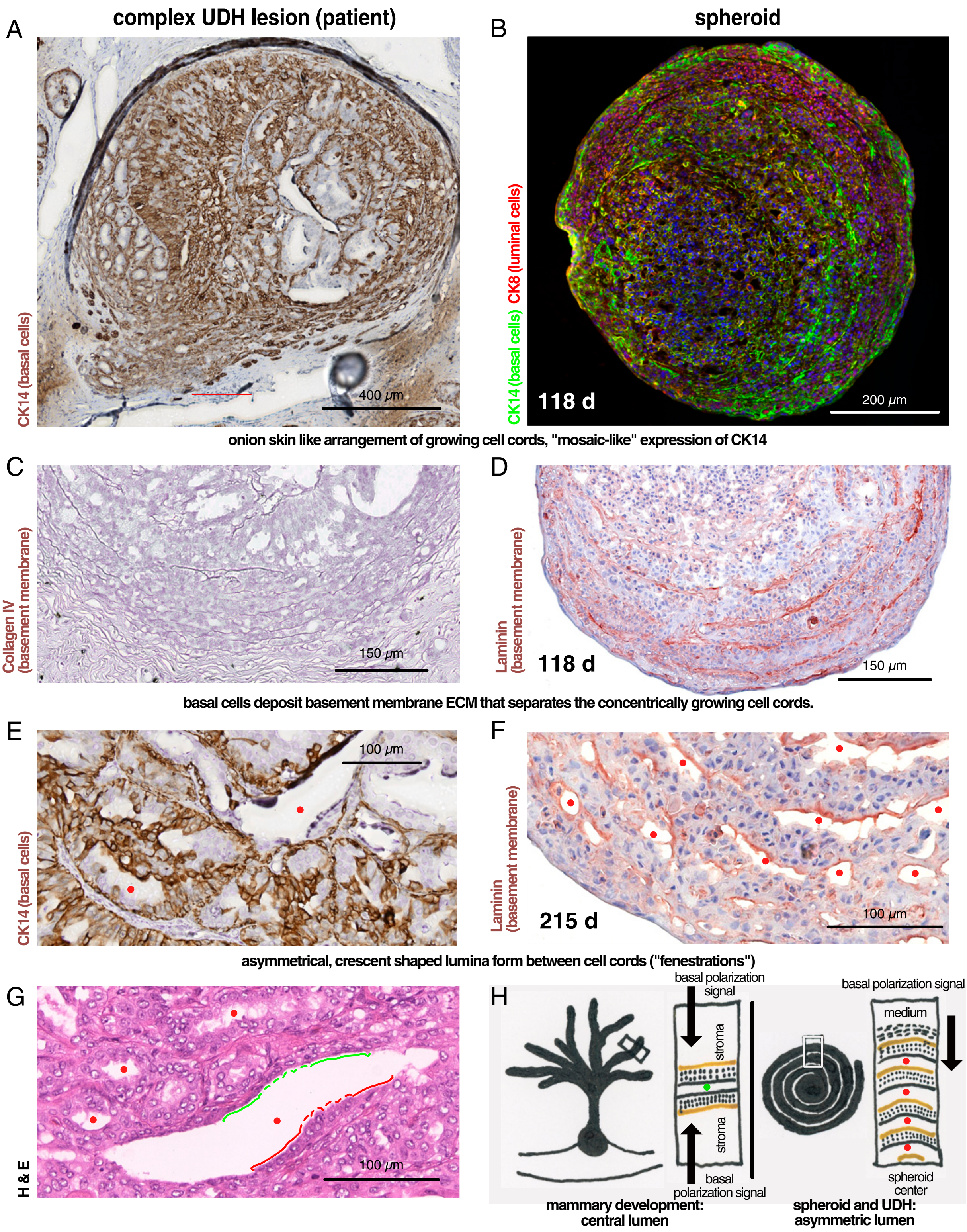

Fig. 7. Comparison of mature spheroids with a complex lesion of UDH. Comparison of a complex UDH lesion with mosaic-like expression of CK14 from a patient (*A*, *C*, *E*, and *G*) with mature spheroids of indicated age (*B*, *D*, and *F*) featuring concentric onion cut surface-like arrangement of cell cords (*C* and *D*) separated by basement membrane component collagen IV (*C*) or laminin (*D*), forming foci of rudimentary (apocrine) epithelium with basal CK14 expression (*E* and *F*) and slit-like lumina (red dots) with matching convex/concave borders that show signs of separation after initial adhesion (*E*–*G*) (compare with Fig. 4). Green and red lines in *G* indicate basal and apical cells with matching outlines, indicating that they were initially adherent to each other. (*H*) A model of how different arrangements of basal polarization signals might influence the position of lumen formation within a cell cord in normal breast development vs. UDH and spheroids.

Table 2. To prepare H14 medium, the following components were added to DMEM/F-12 medium (Hepes buffered, 11330–032; Sigma)

Ingredients	Final concentration	Catalog no.
Insulin	250 ng/mL	I6634-50MG; Sigma
Transferrin	10 μg/mL	T2252-100MG; Sigma
Sodium selenite	2.6 ng/mL	S9133-1MG; Sigma
Estradiol	10^{10} M	E2758-250MG; Sigma
Hydrocortisone	1.4×10^{-6} M	H0888-1G; Sigma
Prolactin	5 μg/mL	L6520-250IU; Sigma
EGF	10 ng/mL	AF-100–15; Peprotech

that lumina can form de novo only within cords, this observation would suggest that all lumina in UDH represent spaces that have not yet been filled by the hyperplastic cell mass (12). In spheroids, however, lumina seem to form between adjacent hyperplastic masses (cords) that were initially adherent (Fig. 4). There are ECM bridges between the two sides, and the "glandular" border is often irregular or slightly serrated as if the two sides had been separated by an active process (Fig. 4 *B–D*). In vivo in UDH, lumina also often show bridges (Fig. 7*E*) and have the characteristic matching convex basal/concave luminal borders that fit together similar to a jigsaw puzzle (Fig. 7*G*). If an active process can generate lumina between rather than within cell cords (as we see in spheroids), a continuous communicating network of lumina can form that consists of both unfilled intraductal space and in addition, "secondary" lumina formed through an active process between adjacent growing cell cords. Based on our observations in spheroids, this seems to be the case in UDH.

The second question is why lumina form in this nonphysiological position between adjacent cell cords. A possible explanation might be that the external polarization signal coming from the medium and acting on the cell cords is asymmetric—stronger on one side. In vivo, during normal formation of lumina in the cord center, polarization signals come from the stroma and ECM (2), and they act symmetrically from all sides. As a result, initially, solid-cell cords develop a lumen through "cord hollowing" in the cord center, where the signals converge. In spheroids and in UDH, however, cell cords are not surrounded by uniform environments, and polarization signals coming from medium/stroma are not equally strong from all sides. In this case, probably, polarization signals do not converge. Instead, the dominant signal propagates until it reaches the cord periphery, and lumina form between cell masses polarized in the same direction (Fig. 7). This nonphysiological constellation could also explain the problems in lumen formation compared with normal development: in spheroids, the tight junction protein ZO-1, which is also involved in formation of adherens junctions (30), is initially localized correctly at the site of lumen formation but becomes mislocalized on the "wrong" basal side of the spheroid lumen rather than the apical cell surfaces (Fig. 4*F*). Formation of similar "half-tubes" with problems in adherens junction formation has been observed during embryonic development of the gut in *Caenorhabditis elegans* after selective experimental removal of primordial cells on only one side of the gut (31). The result was a "half-gut" with an eccentric lumen on one side and preserved direction of polarization of the remaining cells, similar to the lumina in our spheroids and UDH. It will be interesting to see if experimental conditions can be found where spheroid cell cords surrounded by ECM on all sides form a central lumen.

In summary, we show that HMT-3522 S1 spheroids undergo a complex differentiation process that results in tissues morphologically very similar to UDH of the mammary gland. This process shares several interesting properties with embryonic mammary development, which suggests that UDH might result from reactivation of an embryonic-like developmental program in the adult breast. We show that the development of UDH-like lesions in vitro requires an initial switch to collective mode of cell behavior that occurs immediately after aggregation and that contact to Matrigel prevents this switch. We believe that this system is a good in vitro model of UDH and that it will be useful to study UDH biology, lumen formation, and stem cell biology of the mammary gland.

Materials and Methods

Patient Tissue. Archived residual paraffin-embedded tissue left over after diagnostics from two patients with UDH was obtained through ZeBanC (project no. R_251_2019; https://biobank.charite.de), the central biomaterial bank of the Charité Hospital and the Berlin Institute of Health. Anonymized samples were used blinded with respect to patient's data but assigned to diagnosis. The use of tumor tissue for retrospective immunohistochemical analysis was approved by the Charité Ethics Committee (Project EA1/139/05, July 28, 2008, latest amendment 2013). Informed consent from patients for use of biomaterials for research was obtained as part of the institutional treatment contract at Charité.

Spheroid Culture. Spheroids were grown from the cell line HMT-3522 S1 (passages 40–60) provided by Mina Bissell, Lawrence Berkeley National Laboratory, Berkeley, CA. Long-term culture was performed in absence of antibiotics and did not show any signs of contamination, but cells were not specifically tested for mycoplasma contamination.

HMT-3522 S1 cells were grown in 2D on conventional tissue culture dishes (Falcon) in defined serum-free H14 medium as previously published (3). Media components and concentrations are listed in Table 2.

Passaging and freezing protocols provided by the Bissell Laboratory were followed (available at https://www2.lbl.gov/LBL-Programs/lifesciences/BissellLab/protocols.html). Cells were kept at 37 °C with 5% CO_2.

To grow spheroids, 10,000 cells per well were plated on nonadherent, round-bottom 96-well plates (Primesurface, MS-9096UZ; Sumitomo Bakelite) in 150 μL medium and kept at 37 °C with 5% CO_2. One-half of the medium was changed every 1–2 wk. Spheroids also grew and developed normally on 96 nonadhesive U-bottom plates from Thermo Scientific Nunc (174925) and Lipidure (Lipidure-Coat Plate A-U96) but not on the spheroid culture plates from Corning (29443-034 and 10185-094), where the coating does not efficiently prevent adhesion in this cell line and the cells fail to form spheroids.

For Matrigel culture, we used Cultrex BME (without phenol red, reduced growth factor; catalog no. 3433–005-02; PathClear); 96-well plates with optical bottom (655090; Greiner Bio-One) were precoated with 50 μL of ice-cold Matrigel that was allowed to solidify at 37 °C. Then, a preformed spheroid per well was mixed with 150 μL ice-cold Matrigel and pipetted into a precoated well. Again, Matrigel was allowed to solidify at 37 °C, and 100 μL of H-14 medium including EGF was added on top.

Immunohistochemistry. Spheroids were embedded in O.C.T. compound (Sakura Finetek), and serial 5-μm-thick frozen sections were prepared for histopathological analysis. The frozen sections were fixed with the BD Cytofix/Cytoperm Fixation/Permeabilization Kit (catalog no. 554714; BD) at room temperature for 15 min followed by three wash steps in PBS (5 min each). Next, the sections were treated with 0.3% H_2O_2 in distilled water to suppress endogenous peroxidase activity, and then, they were blocked and stained with the antibodies listed in Table 3.

Table 3. Antibodies used for spheroid immunohistochemistry

Antibody	Company	Incubation/dilution	Catalog no.	Company	Secondary	Blocking agent
Laminin	abcam	1:100 O/N	ab11575	Vector	BA1000	4% Goat
E-Cadherin	CST	1:100 O/N	3195	Vector	BA1000	4% Goat
Ki67 (B56)	BD	1:25 O/N	550609	Vector	BA2000	4% Horse

O/N, overnight.

Table 4. For immunofluorescence staining, the following primary antibodies were used

Antigen	Host species	Catalog no.	Clone	Company
E-cadherin	Rabbit monoclonal	3195	24E10	Cell Signaling
Laminin	Rabbit polyclonal	ab11575	NA	Abcam
CK14	Rabbit polyclonal	905301	NA	Biolegend/Covance
CK8	Mouse IgG2a, λ	904801	1E8	Biolegend
Pancytokeratin	Mouse IgG1, κ	628601	C-11	Biolegend
p63	Mouse IgG2a, κ	CM163	4A4	DAKO
Na^+/K^+ ATPase (membrane marker)	Mouse IgG2a, κ		a6F	http://dshb.biology.uiowa.edu
ZO-1	Rabbit polyclonal	61–7300	NA	ThermoFisher

NA, not applicable.

After washing the sections in PBS three times for 5 min each, secondary antibodies followed by the Vectastain ABC kit (Vector Laboratories) were applied. A 3-amino-9-ethylcarbazole substrate (Dako) was used for color development, and all of the sections were counterstained with Harris hematoxylin (Sigma-Aldrich). The slides were covered with glass coverslips using aqueous mounting medium (50212451; Fisher), and images were captured using NanoZoomer 2.0RS (Hamamatsu).

Antibodies used for immunofluorescence staining of spheroids are listed in Table 4. Fluorescence images of spheroids were aqcuired on a widefield inverted Nikon Ti fluorescence microscope equipped with a Hamamatsu ORCA-ER cooled CCD camera controlled by MetaMorph software at 20× magnification.

Patient tissues were stained according to standard manufacturer protocols for diagnostics on automated Ventana Benchmark XT stainers with the following antibodies:

Collagen IV, Cell Marque, diluted 1:25, catalog no.44261, clone CIV22; and

Keratin 14, Biogenex, diluted 1:25, catalog no. AM146, clone LL002.

Electron Microscopy. Spheroids were fixed in 3% gluraldehyde in BRB80 buffer prewarmed to 37 °C for 20 min to 2 h depending on the size and then, rinsed in BRB80 twice before postfixation with 1% osmium with 0.8% $K_3Fe(CN)_6$ in 0.1 M cacodylate buffer, pH 7.4, for 15–30 min on ice in the hood. Samples were then rinsed twice with buffer and twice with distilled water. They were then en block stained with 1% aqueous uranyl acetate (filtered) overnight at 4 °C in the dark.

The next day, samples were rinsed in distilled water and dehydrated in an ethanol series using the progressive lowering of temperature method (35 and 50% at 4 °C, 50 and 80% at −20 °C, and 95 and 100% at −40 °C). At room temperature, they were rinsed with fresh 100% ethanol and 100% propylene oxide before infiltration with propylene oxide-epon araldite solutions (2:1, 1:2) and then, 100% epon araldite. Samples were mounted and polymerized at 65 °C for 48 h. Individual spheroids were remounted for serial thin sectioning (75 nm) on a Reichert Ultracut S microtome. Sections were picked up on formvar-coated slot grids, and they were viewed and imaged on a Tecnai G2 Spirit Biotwin TEM equipped with an AMT 2k CCD camera.

ACKNOWLEDGMENTS. We thank Mina Bissell (Lawrence Berkeley National Laboratory) for providing the HMT-3522 S1 cell line, advice, and support. We are grateful for detailed descriptions of UDH (9, 12, 16) and mammary embryonic development (22). We thank Carsten Denkert for generous support, advice, and lab space. We are grateful for the support of The Nikon Imaging Center at Harvard Medical School. S.F. was supported by Research Fellowship FL 820/1-1 from the Deutsche Forschungsgemeinschaft. This project was supported by US NIH Grants R01-CA164448 (to R.W.), S10RR0266360 (to R.W.), and P01-CA139980 (to T.J.M.).

1. Huebner RJ, Ewald AJ (2014) Cellular foundations of mammary tubulogenesis. *Semin Cell Dev Biol* 31:124–131.
2. Inman JL, Robertson C, Mott JD, Bissell MJ (2015) Mammary gland development: Cell fate specification, stem cells and the microenvironment. *Development* 142:1028–1042.
3. Blaschke RJ, Howlett AR, Desprez PY, Petersen OW, Bissell MJ (1994) Cell differentiation by extracellular matrix components. *Methods Enzymol* 245:535–556.
4. Hebner C, Weaver VM, Debnath J (2008) Modeling morphogenesis and oncogenesis in three-dimensional breast epithelial cultures. *Annu Rev Pathol* 3:313–339.
5. Weaver VM, Howlett AR, Langton-Webster B, Petersen OW, Bissell MJ (1995) The development of a functionally relevant cell culture model of progressive human breast cancer. *Semin Cancer Biol* 6:175–184.
6. Fata JE, et al. (2007) The MAPK(ERK-1,2) pathway integrates distinct and antagonistic signals from TGFalpha and FGF7 in morphogenesis of mouse mammary epithelium. *Dev Biol* 306:193–207.
7. Ewald AJ, Brenot A, Duong M, Chan BS, Werb Z (2008) Collective epithelial migration and cell rearrangements drive mammary branching morphogenesis. *Dev Cell* 14:570–581.
8. Ewald AJ, et al. (2012) Mammary collective cell migration involves transient loss of epithelial features and individual cell migration within the epithelium. *J Cell Sci* 125:2638–2654.
9. Azzopardi JG (1979) "Epitheliosis." *Problems in Breast Pathology*, eds Azzopardi JF, Ahmed A, Millis RR (WB Saunders, Philadelphia), pp 113–127.
10. Tavassoli FA, Devilee P (2003) *Pathology and Genetics of Tumours of the Breast and Female Genital Organs*, World Health Organization Classification of Tumours (IARC Press, Lyon, France).
11. Eusebi V, Millis RR (2010) Epitheliosis, infiltrating epitheliosis, and radial scar. *Semin Diagn Pathol* 27:5–12.
12. Koerner FC (2004) Epithelial proliferations of ductal type. *Semin Diagn Pathol* 21:10–17.
13. Hartmann LC, et al. (2005) Benign breast disease and the risk of breast cancer. *N Engl J Med* 353:229–237.
14. Sutherland RM, McCredie JA, Inch WR (1971) Growth of multicell spheroids in tissue culture as a model of nodular carcinomas. *J Natl Cancer Inst* 46:113–120.
15. Briand P, Petersen OW, Van Deurs B (1987) A new diploid nontumorigenic human breast epithelial cell line isolated and propagated in chemically defined medium. *In Vitro Cell Dev Biol* 23:181–188.
16. Boecker W, et al. (2002) Usual ductal hyperplasia of the breast is a committed stem (progenitor) cell lesion distinct from atypical ductal hyperplasia and ductal carcinoma in situ. *J Pathol* 198:458–467.
17. Freyer JP (1988) Role of necrosis in regulating the growth saturation of multicellular spheroids. *Cancer Res* 48:2432–2439.
18. Boecker W, Dabbs DJ (2012) Fibrocystic change and usual epithelial hyperplasia of ductal type. *Breast Pathology*, ed Dabbs DJ (Elsevier, New York), pp 324–344.
19. Ohuchi N, Abe R, Takahashi T, Tezuka F, Kyogoku M (1985) Three-dimensional atypical structure in intraductal carcinoma differentiating from papilloma and papillomatosis of the breast. *Breast Cancer Res Treat* 5:57–65.
20. Bussard KM, Smith GH (2012) Human breast cancer cells are redirected to mammary epithelial cells upon interaction with the regenerating mammary gland microenvironment in-vivo. *PLoS One* 7:e49221.
21. Boulanger CA, et al. (2013) Embryonic stem cells are redirected to non-tumorigenic epithelial cell fate by interaction with the mammary microenvironment. *PLoS One* 8:e62019.
22. Hogg NA, Harrison CJ, Tickle C (1983) Lumen formation in the developing mouse mammary gland. *J Embryol Exp Morphol* 73:39–57.
23. Boras-Granic K, Dann P, Wysolmerski JJ (2014) Embryonic cells contribute directly to the quiescent stem cell population in the adult mouse mammary gland. *Breast Cancer Res* 16:487.
24. Zvelebil M, et al. (2013) Embryonic mammary signature subsets are activated in Brca1-/- and basal-like breast cancers. *Breast Cancer Res* 15:R25.
25. Sun P, Yuan Y, Li A, Li B, Dai X (2010) Cytokeratin expression during mouse embryonic and early postnatal mammary gland development. *Histochem Cell Biol* 133:213–221.
26. Friedrichs N, Steiner S, Buettner R, Knoepfle G (2007) Immunohistochemical expression patterns of AP2alpha and AP2gamma in the developing fetal human breast. *Histopathology* 51:814–823.
27. Hughes ES (1950) The development of the mammary gland: Arris and Gale Lecture, delivered at the Royal College of Surgeons of England on 25th October, 1949. *Ann R Coll Surg Engl* 6:99–119.
28. Gusterson BA, Stein T (2012) Human breast development. *Semin Cell Dev Biol* 23:567–573.
29. Standring S (2008) *Gray's Anatomy: The Anatomical Basis of Clinical Practice*, eds Standring S, Gray H (Churchill Livingstone/Elsevier, Edinburgh), pp 915–938.
30. Ikenouchi J, Umeda K, Tsukita S, Furuse M, Tsukita S (2007) Requirement of ZO-1 for the formation of belt-like adherens junctions during epithelial cell polarization. *J Cell Biol* 176:779–786.
31. Leung B, Hermann GJ, Priess JR (1999) Organogenesis of the Caenorhabditis elegans intestine. *Dev Biol* 216:114–134.